

ANN Based Control and Estimation of Direct Torque Controlled Induction Motor Drive

Rajesh Kumar¹ R.A. Gupta² S.V. Bhangale³ Himanshu Gothwal⁴

Abstract – Direct Torque Control (DTC) of Induction Motor drive has quick torque response without complex orientation transformation and inner loop current control. Although DTC has some drawbacks, such as the torque and flux ripple. The control scheme performance relies on the accurate selection of the switching voltage vector. This paper proposed simple structured neural network based new identification method for flux position estimation, sector selection and stator voltage vector selection for induction motors using direct torque control (DTC) method. The ANN based speed controller has been introduced to achieve good dynamic performance of induction motor drive. The Levenberg-Marquardt back-propagation technique has been used to train the neural network. Proposed simple structured network facilitates a short training and processing times. The stator flux is estimated by using the modified integration with amplitude limiter algorithms to overcome drawbacks of pure integrator. The conventional flux position estimator, sector selector and stator voltage vector selector based modified direct torque control (MDTC) scheme compared with the proposed scheme and the results are validated through both by simulation and experimentation.

Keywords – ANN based speed controller, direct torque control (DTC), flux position estimator

I. INTRODUCTION

The induction motor is very popular in variable speed drives due to its well known advantages of simple construction, ruggedness, and inexpensive and available at all power ratings. Progress in the field of power electronics and microelectronics enables the application of induction motors for high-performance drives where traditionally only DC motors were applied. Thanks to sophisticated control methods, induction motor drives offer the same control capabilities as high performance four quadrant DC drives. A major revolution in the area of induction motor control was invention of field-oriented control (FOC) or vector control by Blaschke [1] and Hasse [2].

In vector control methods, it is necessary to determine correctly the orientation of the rotor flux vector, lack of which leads to poor response of the drive. The main drawback of FOC scheme is the complexity. The new technique was developed to find out different solutions for the induction motor torque control, reducing the complexity of FOC schemes known as Direct Torque control (DTC).

Direct Torque control (DTC) for induction motor was introduced about twenty years ago by Japanese and German researchers Takahashi and Noguchi [3]-[4]. DTC was considered as an alternative to the field oriented control scheme to overcome the weakness of scheme.

In DTC, the torque and flux are directly controlled by using the selection of optimum voltage vectors. The switching logic control facilitate the generation of the stator voltage space vector, with a suitable choice of the switching pattern of the inverter, on the basis of the knowledge of the sector (supplied by the stator flux model block) in which the stator flux lies, and of the amplitudes of the stator flux and the torque. The sector identification depends on the accurate estimation of stator flux position. Novel artificial-intelligence-based stator flux estimator for induction motor has been proposed by [5].

The ANNs are capable of learning the desired mapping between the inputs and outputs signals of the system without knowing the exact mathematical model of the system. Since the ANNs do not use the mathematical model of the system, the same. The ANNs are excellent estimators in non linear systems [6] - [8]. Various ANN based control strategies have been developed for direct torque control induction motor drive to overcome the scheme drawback [9] - [11].

In this paper, neural network flux position estimation, sector selection and switching vector selection scheme proposed, and ANN based speed controller used to reduce the current ripple by regulating the switching frequency, are proposed. Total harmonic distortion (THD) of the stator current analysis has been also presented in this work.

The organization of this paper goes on in the following order. In Section II, it will be presented the Mathematical model and basic concept of DTC for induction motor drive. In Section III and IV it will be described flux estimation algorithm and artificial neural networks and implementation of ANN to the DTC scheme. The simulation and experimental results will be presented in Section V and VI for the proposed scheme validation. In Sections VII, it will be presented the conclusions of this work.

II. MATHEMATICAL MODEL OF INDUCTION MOTOR AND BASIC CONCEPT OF DTC

The dynamic model of the induction motor is derived by transforming the three phase quantities into two phase direct and quadrature axes quantities. The mathematical model in compact form can be given in the stationary reference frame as follows [12].

The paper first received 21 Aug. 2008 and in revised form 3 Nov 2008.
Digital ref: A170401208

^{1,2,3,4} Department of Electrical Engineering, Malaviya National Institute of Technology, JLN Marg, Jaipur, India, E-mail: ¹rkumar_mnit@rediffmail.com, E-mail: ²rag_mnit@rediffmail.com, E-mail: ³bhangale_sv@yahoo.com

$$\begin{pmatrix} v_{ds} \\ v_{qs} \\ v_{dr} \\ v_{qr} \end{pmatrix} = \begin{pmatrix} R_s + L_s p & 0 & L_m p & 0 \\ 0 & R_s + L_s p & 0 & L_m p \\ L_m p & \omega_r L_m & R_r + L_r p & \omega_r L_r \\ -\omega_r L_m & L_m p & -\omega_r L_r & R_r + L_r p \end{pmatrix} \begin{pmatrix} i_{ds} \\ i_{qs} \\ i_{dr} \\ i_{qr} \end{pmatrix} \quad (1)$$

$$\psi_{ds} = L_s i_{ds} + L_r i_{dr}, \quad \Psi_{qs} = L_s i_{qs} + L_r i_{qr} \quad (2)$$

$$\psi_{dr} = L_r i_{dr} + L_s i_{ds}, \quad \Psi_{qr} = L_r i_{qr} + L_s i_{qs} \quad (3)$$

where v_{ds} , v_{qs} , i_{ds} , i_{qs} , R_s , L_s , R_r , L_r , L_m , Ψ_{ds} , Ψ_{qs} , Ψ_{dr} , Ψ_{qr} and θ_r are the d-q axes voltages and currents, stator resistance, stator inductance, rotor resistance, rotor inductance, mutual inductance between the stator and rotor windings, stator flux linkages, rotor flux linkages and the rotor position respectively.

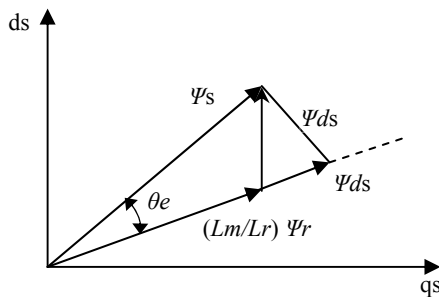


Fig. 1: Stator and rotor flux-linkage space vectors.

The electromagnetic torque obtained from machine flux linkages and currents is as:

$$T_e = \frac{3}{2} \frac{P}{2} L_m (i_{qs} \psi_{dr} - i_{ds} \psi_{qr}) \quad (4)$$

where T_e , P , Ψ_{dr} , Ψ_{qr} are the electromagnetic torque, number of poles, rotor d-q axes fluxes respectively.

The electromagnetic torque equation can also be obtained in stationary reference frame as:

$$T_e = \frac{3}{2} \frac{P}{2} \frac{L_m}{\sigma L_r L_s} |\psi_r| |\psi_s| \sin \theta_e \quad (5)$$

where $\sigma = \text{Leakage coefficient} = 1 - \left(\frac{L_m^2}{L_s L_r} \right)$

The angle between the stator and rotor flux linkage space vectors is θ_e as shown in Fig. 1.

The stator flux linkage, voltage and torque equations in d-q axis stationary reference frame can be obtained as follows

$$v_{ds} = R_s i_{ds} + p \psi_{ds} \quad (6)$$

$$v_{qs} = R_s i_{qs} + p \psi_{qs} \quad (7)$$

$$\psi_{ds} = \int (v_{ds} - R_s i_{ds}) dt \quad (8)$$

$$\psi_{qs} = \int (v_{qs} - R_s i_{qs}) dt \quad (9)$$

$$\psi_s = \sqrt{\psi_{ds}^2 + \psi_{qs}^2} \quad (10)$$

$$\theta_e = \tan^{-1} \left(\frac{\psi_{qs}}{\psi_{ds}} \right) \quad (11)$$

From equation (5) it is clear that the motor torque can be varied by changing the rotor or stator flux vectors. The rotor time constant of a standard squirrel-cage induction machine is very large, thus the rotor flux linkage changes slowly compared to the stator flux linkage. However, during a short transient, the rotor flux is almost unchanged. Thus rapid changes of the electromagnetic torque can be produced by rotating the stator flux in the required direction, which is determined by the torque command. On the other hand the stator flux can instantaneously be accelerated or decelerated by applying proper stator voltage phasors. Depending on the position of the stator flux, it is possible to switch on the suitable voltage vectors to control both flux and torque.

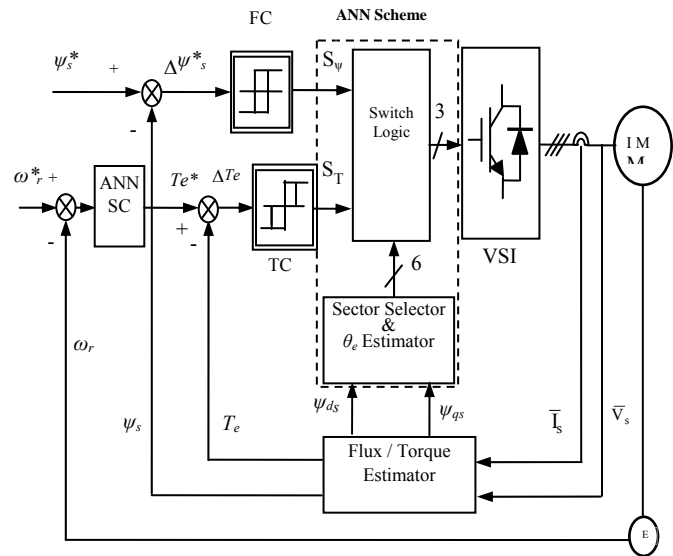


Fig. 2: Proposed ANN based DTC scheme

The switching logic given below in the table 1 is developed from the output signals of hysteresis comparators; represent the increment (decrement) of the flux (torque).

Table 1: Switching logic

Conditions for Flux	S_ψ
$ \psi_s \leq \psi_s^* - \Delta\psi_s $	1
$ \psi_s \geq \psi_s^* + \Delta\psi_s $	0
Conditions for Torque	S_T
$ T_e \leq T_e^* - \Delta T_e $	1
$ T_e = T_e^* $	0
$ T_e \geq T_e^* + \Delta T_e $	-1

The first sector of -30° to 30° in conventional, is taken as 0° to 60° and the new modified optimal switching voltage vector table is given in table 2, where k (i.e. $k = 1, 2, \dots, 6$) indicates the sector position of stator flux.

Table 2: Voltage switching vector table (MDTC)

	$ \psi_s \uparrow (\Delta\psi_s = 1)$	$ \psi_s \downarrow (\Delta\psi_s = 0)$
$T_e \uparrow (\Delta T_e = 1)$	v_{k+1}	v_{k-2}
$T_e \uparrow (\Delta T_e = 0)$	v_7 OR v_8	v_7 OR v_8
$T_e \downarrow (\Delta T_e = -1)$	v_{k+5}	v_{k+4}

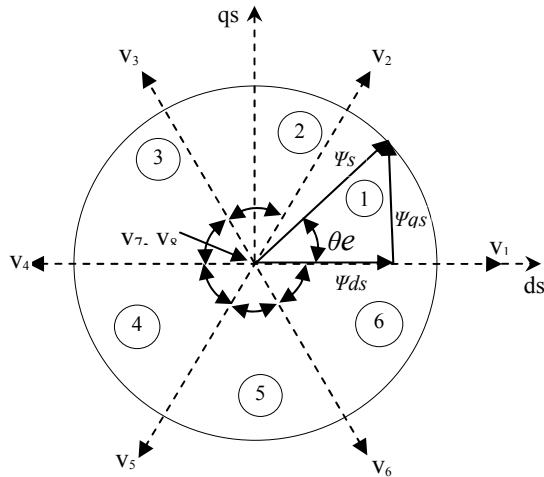


Fig. 3: Position of stator flux vector in the space-vector plane (MDTC).

III. STATOR FLUX ESTIMATOR ALGORITHM

In (8) and (9), pure integrators are applied to estimate the stator flux. Notably, initial value error and dc-offset problems exist herein. To improve these problems, solution proposed to use the low-pass filter that has the input-output relation given by a newly proposed integration algorithm is used [13], the Simulink model is developed for stator flux estimation algorithm as shown in Fig. 4.

The input output relation of the low pass filter is given by

$$y = \frac{1}{s + \omega_c} \cdot x \tag{12}$$

By choosing a low value of cut off frequency ω_c leads to a better integration, but higher dc bias. A higher value of cutoff frequency ω_c changes the integration output. The d-q axis stator fluxes in the stationary reference frame are mainly computed by the integration of back emf in the d-q frame which can be obtained by the abc to d-q transformation. The stator flux amplitude and angle are calculated from (10) and (11), the absolute value of flux is dc bias signal obtained from the flux limiter block output. These signals are transferred into original form by using the Polar to Cartesian. This algorithm is suitable for the constant flux operation.

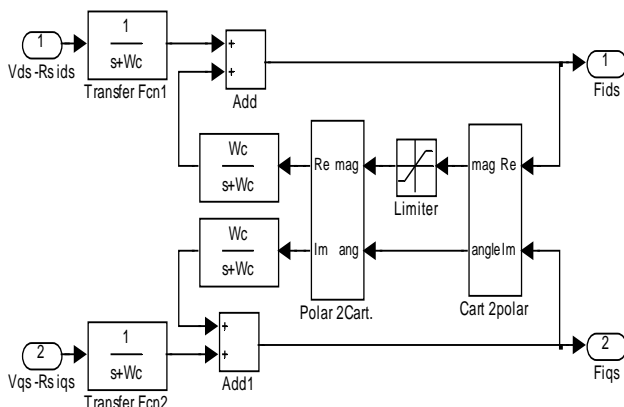


Fig. 4: Simulink model of integration method for stator flux estimation.

IV. ARTIFICIAL NEURAL NETWORK BASED ESTIMATOR AND CONTROLLER

ANN has a very significant role in the field of artificial intelligence. The artificial neurons learn from the data fed to them and keep on decreasing the error during training time and once trained properly, their results are very much same to the results required from them, thus referred to as universal approximators [14]. The most popular neural network used by researchers are the multilayer feed forward neural network trained by the back propagation algorithm [15]. There are different kinds of neural networks classified according to operations they perform or the way of interconnection of neurons. Some approaches use neural networks for parameters estimation of electrical machines in feedback control of their speeds [16, 17].

A. ANN based voltage vector estimator

Here we have used a feed forward neural network to select the voltage vector. For this purpose different configurations of networks were used and the best configured network is proposed and this scheme is depicted in the Fig. 2. The relation of variables used in the proposed scheme is as shown in Fig. 3. There are three neural networks. First is to estimate the value of stator flux position, θ_e as shown in the Fig. 5. This is the angle between the stator flux and the rotor flux. It is a two input-one output feed-forward network with three layers. The input layer has 6 neurons of hyperbolic tangent sigmoid transfer function, first hidden layer has 4 neurons of log sigmoid transfer function and the output layer has 1 neuron of linear function. The necessary steps to adjust these weights associated with the hidden neurons can be made through the training of the neurons. Levenberg-Marquardt back-propagation method is used here for training the network [18]. The inputs given are 'd-axis stator flux' and 'q-axis stator flux'.

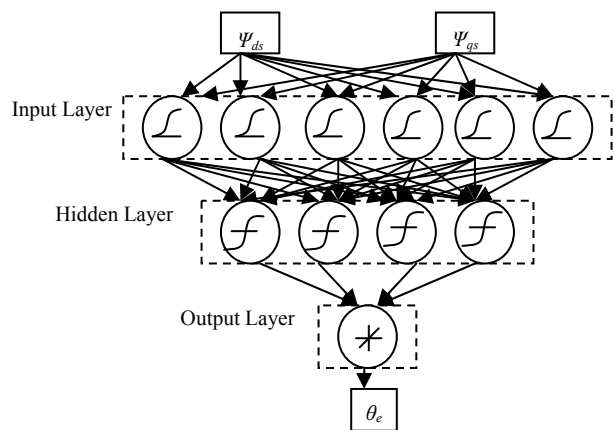


Fig. 5: Feed forward ANN for theta estimation.

Second neural network is used to determine the sector number for the estimated value of θ_e . There are total of six sectors, each sector of 60 degree. Again three layers of neurons are used but with a 5-4-1 feed forward configuration as shown in Fig. 6. Input layer is of log sigmoid transfer function, hidden layer is of hyperbolic

tangent sigmoid function and the output layer is of linear transfer function. The training method used was Levenberg-Marquardt back-propagation. The input given is the angle theta since sector selection is purely based on theta.

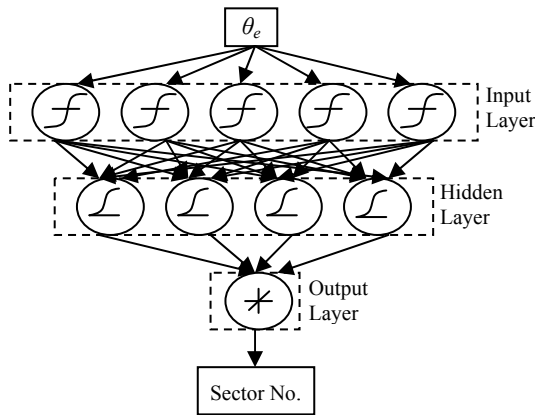


Fig. 6: Feed forward ANN for sector selection

Last neural network is for the selection of voltage vector as given in Fig. 7, which is based on three inputs, flux, torque and the sector. Network taken this time is a 3-5-1 feed forward network with first layer of log sigmoid transfer function, second layer of hyperbolic tangent sigmoid transfer function and third layer of linear transfer function. Training method used was again Levenberg-Marquardt back-propagation. All the three neural networks were trained to performance 0.00001 mse. Here mse is a network performance function and it measures the network's performance according to the mean of squared errors (mse).

The back-propagation algorithm is used to train the neural networks. The training function used is Levenberg-Marquardt back-propagation, it updates weights and bias values according to Levenberg-Marquardt optimization.

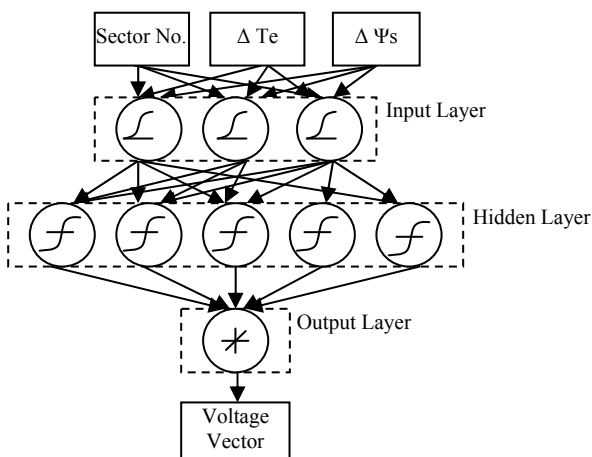


Fig. 7: Feed forward ANN for sector selection

As soon as the training procedure is over, the neural network gives almost the same output pattern for the same or nearby values of input. This tendency of the neural networks which approximates the output for new input data is the reason for which they are used as intelligent systems.

B. ANN Speed Controller

The input and output of the ANN controller can be obtained from the PI controller input output and which can be written as:

$$Y(s) = X(s) \left(K_p + \frac{K_i}{s} \right) \tag{13}$$

Where X(s) is the input and Y(s) is the output of PI controller, K_p and K_i are the proportional and integral gain constants.

The equation (13) can be written in the difference form as:

$$y(n) = y(n-1) + K_p [x(n) - X(n-1)] + K_i x(n) \tag{14}$$

Where n is present time constant and (n-1) is previous time constant. The equation for speed controller can be obtained as:

$$x(n) = \omega_{ref}(n) - \omega_r(n) \tag{15}$$

y(n) is the output of speed controller which is the controlling torque for the present control scheme of induction motor drive. The ANN based speed controller (ANNSC) structure is as shown in Fig. 8.

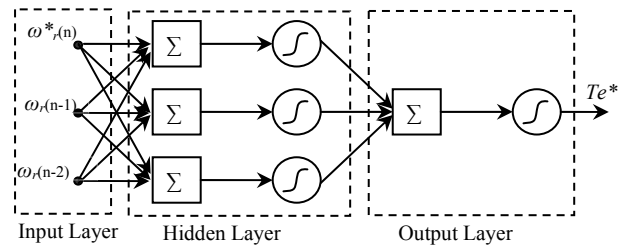


Fig. 8: Feed forward ANN speed controller

V. SIMULATION RESULTS

The results of simulation obtained in this work are for the induction motor of 3 HP and parameters as given in appendix. The machine model is implemented for modified DTC scheme and proposed ANN based DTC scheme using Matlab /Simulink.

First the MDTC scheme is applied to the induction motor to check the performance under no load and then switch to full load (12-Nm) condition at 0.4 sec. The speed reversal has been applied at 0.55 sec and the results of stator currents for all conditions are presented in Fig. 9 (a). Fig. 9 (c) and Fig. 9 (e) shows the torque and the speed response under steady state and transient condition for conventional DTC scheme. Fig. 9 (b) and Fig. 9 (d) shows the results of the stator current and torque, (zoomed for comparison) which present more ripples.

The results for ANN based DTC scheme under the same loading conditions, speed reversal as in case of MDTC scheme are presented in Fig. 10 (a) and Fig. 10 (e). The torque ripples and stator current harmonic content are reduced as seen in the results. Fig. 10 (b) and Fig. 10 (d) shows that the ripples in the stator current and torque is comparatively less which supports accuracy in the ANN based estimator and validation for ANN based DTC scheme. Fig. 10 (f) shows the smoothness in the flux plot of the proposed scheme as compared to its counterpart of MDTC scheme as in Fig. 9 (f). For comparison purposes, the harmonic current analysis is performed at spectra frequency of 1000 Hz and the fundamental current

frequency of 50 Hz. The harmonic analysis is carried for Fig. 9 (a) and Fig. 10 (a) under no load (0.1 sec to 0.3 sec period) and load (0.4 sec to 0.5 sec period) condition and results are shown in Fig. 11 and Fig. 12. Comparative harmonic analysis results during no-load and load operation have been depicted in Table 3.

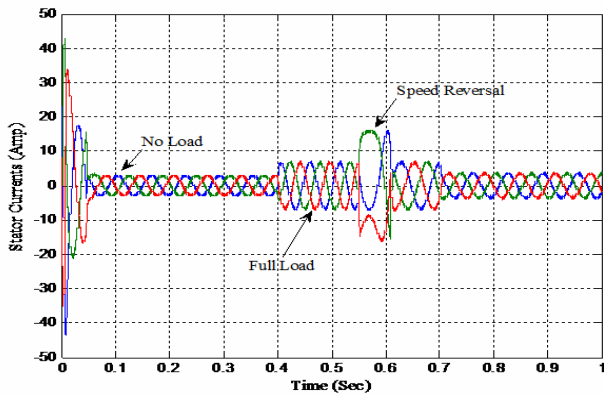


Fig. 9 (a): Stator current response of MDTC scheme for all operating conditions.

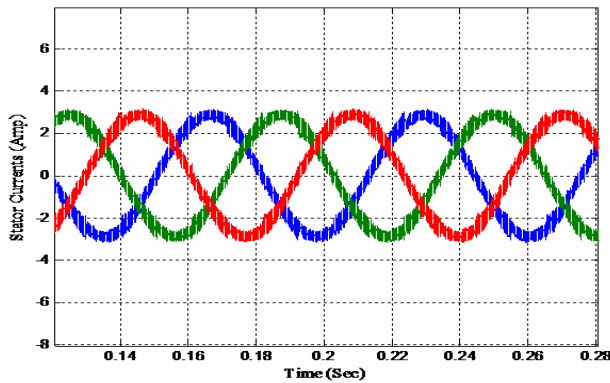


Fig. 9 (b): Stator current (Zoomed) response of MDTC scheme for no load condition

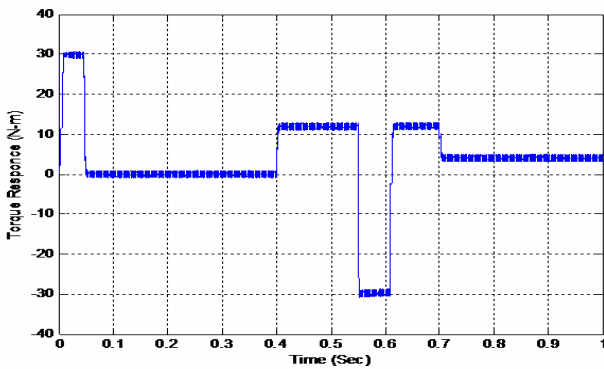


Fig. 9 (c): Torque response of MDTC scheme for all conditions.

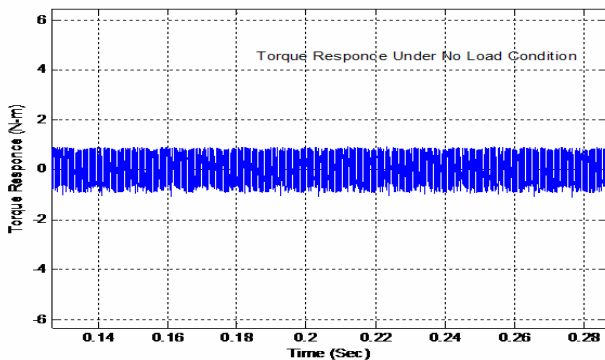


Fig. 9 (d): Zoomed torque response for time interval 0.14 sec to 0.28 sec of Fig.9 (c).

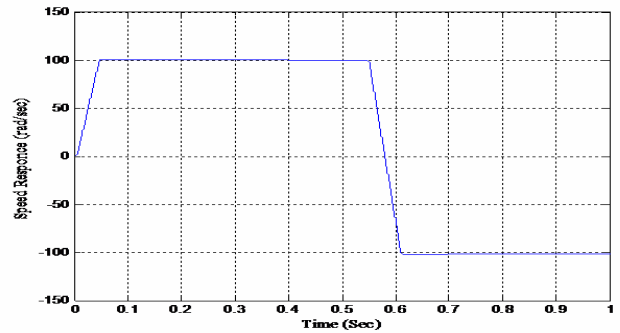


Fig. 9 (e): Speed response of conventional DTC scheme

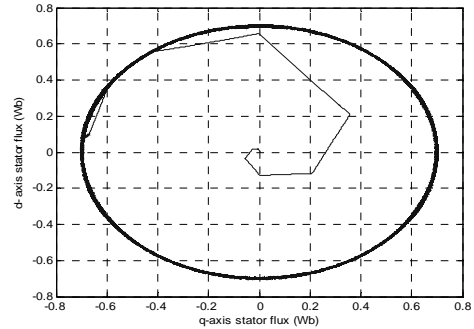


Fig. 9 (f): d-q-axis stator flux plot (MDTC Scheme).

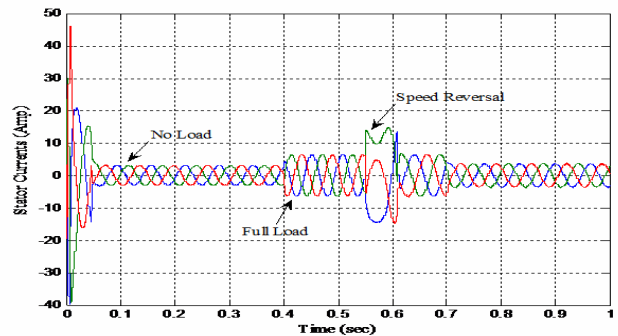


Fig. 10 (a): Stator current response of ANN based DTC scheme for all operating conditions.

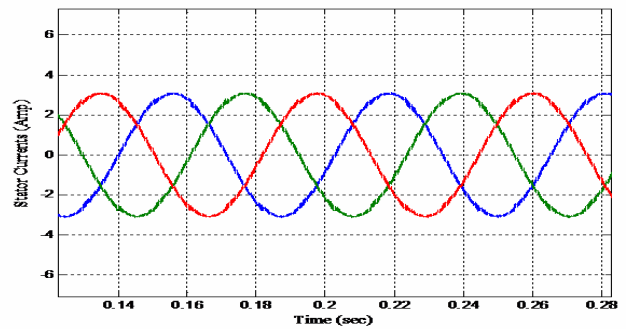


Fig. 10 (b): Stator current (Zoomed) response of ANN based DTC scheme for no load condition

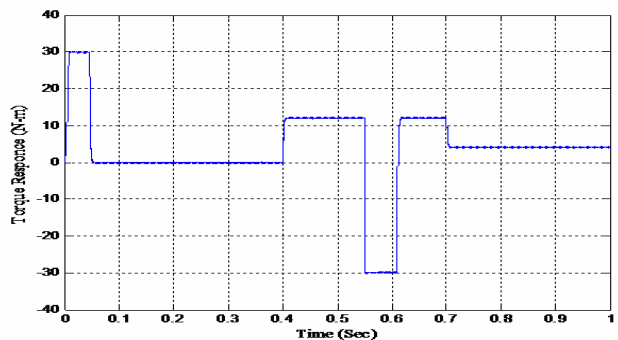


Fig. 10 (c): Torque response of ANN based DTC scheme for all conditions

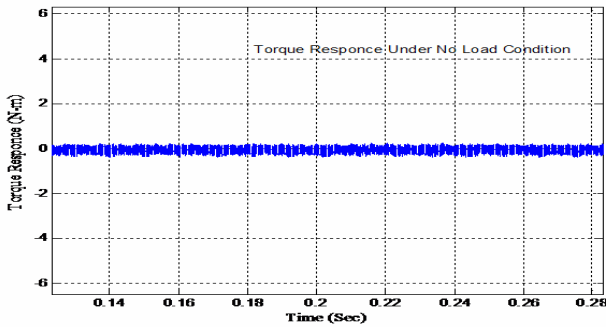


Fig. 10 (d): Zoomed torque response for time interval 0.14 sec to 0.28 sec of Fig. 10 (c).

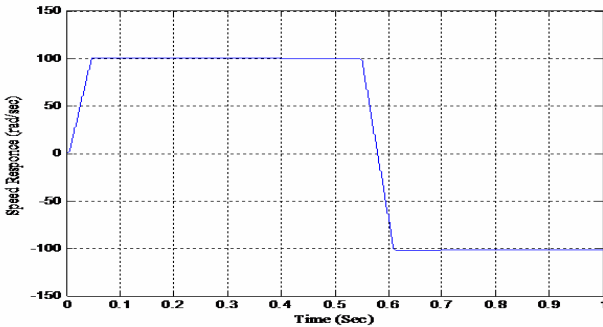


Fig. 10(e): Speed response of ANN based DTC scheme

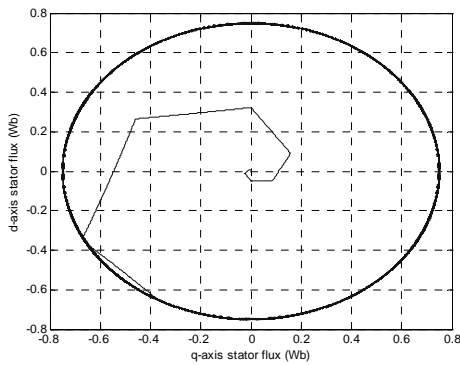
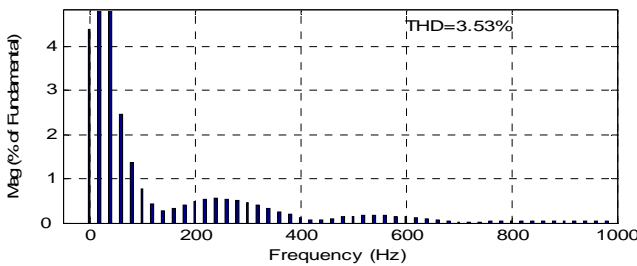
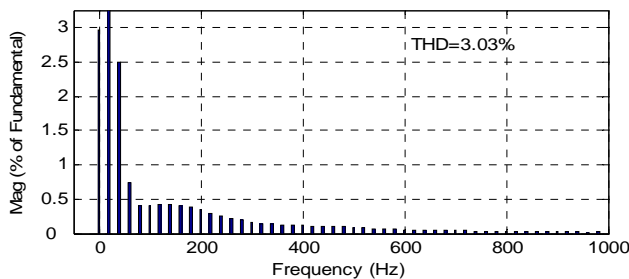


Fig. 10 (f): d-q-axis stator flux plot (ANN based DTC scheme)

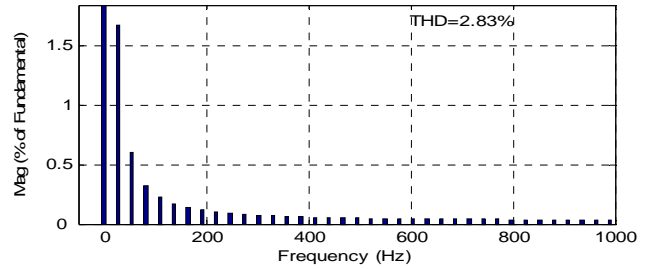


(a)

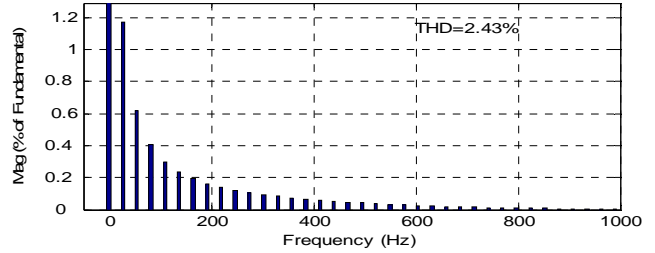


(b)

Fig. 11: Harmonic spectrum of stator current under no load (a) and load (b) condition for MDTC



(a)



(b)

Fig. 12: Harmonic spectrum of stator current under no load (a) and load (b) condition for ANN based DTC

Table 3: Comparison of total harmonic distortion for the modified DTC and ANN based DTC schemes

Control Scheme	THD (%) of Stator current (Amp)	
	No load	load
Modified DTC	3.53%	3.03%
ANN based DTC	2.83%	2.43%

VI. EXPERIMENTAL RESULTS

In order to make the experimental validation of the effectiveness of the proposed DTC scheme for torque ripple reduction, a DSP-based induction motor drive system has been built. The experimental setup includes a fully digital controlled IGBT 5kVA Semikron make inverter and a 2.2-kW, 415-V, 50-Hz, four-pole induction motor. The control scheme has been implemented on dSPACE controller board DS-1104 which consist a DSP processor MPC8240 of 250 MHz. The dSPACE has 4 multiplexed channel, 16-bit sample and hold ADC, 4 parallel channels, 12-bit sample and hold ADC and 8 channel of digital to analog converter (DAC), with 16-bit resolution. The induction motor has the same parameters applied in simulation. The machine currents i_a and i_b sensed by LEM LA 55-P current sensor and voltage sensor LEM LV 100-1000V used to sense the dc bus voltage these signals were interfaced into the controller through an analog to digital converter (A/D) which is separate peripheral unit of controller board. The photo of experimental set is shown in Fig. 13. The controller sampling time set to 0.0001 sec and DSP board was controlled with a PC.

Fig. 14 (b) shows the corresponding waveform for the of d-q axis stator fluxes reflect the reduction in ripples and confirms the effectiveness of flux ripple reduction to decrease the torque ripple as depicted in Fig. 16 (b) .

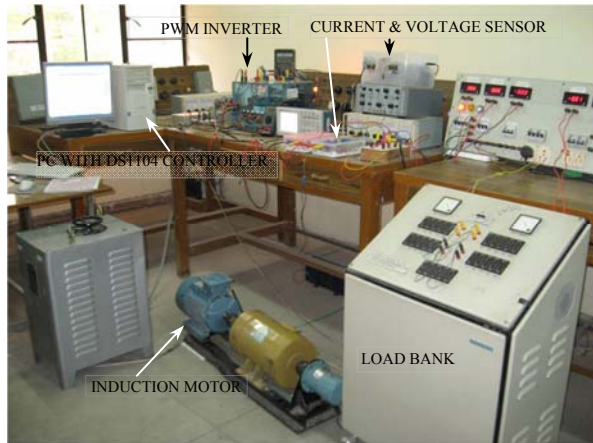


Fig. 13: Photo of experimental setup

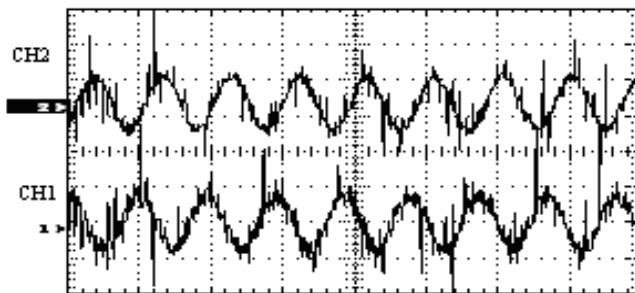


Fig. 14 (a)

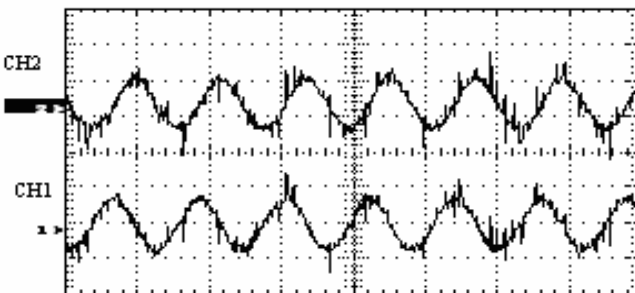


Fig. 14 (b)

Experimental response of the d axis stator flux (upper trace) and q axis stator flux (lower trace) (a) for MDTC. (b) ANN based DTC (in y axis flux 1 Wb/div, in x axis 50 ms/div)

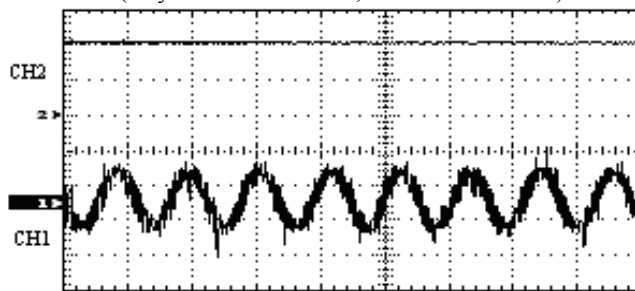


Fig. 15 (a)

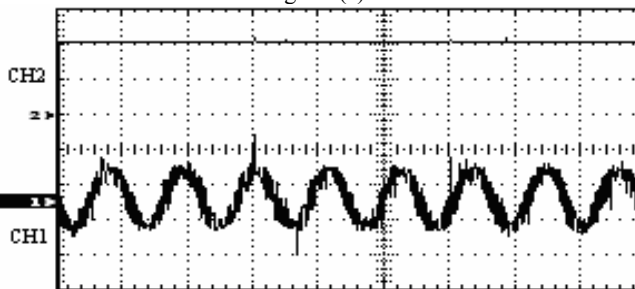


Fig. 15 (b)

Experimental response of the rotor speed (upper trace) & stator current i_a (lower trace) (a) for MDTC. (b) ANN based DTC $i_a = 3A/div$ rotor speed = 50 (rad/sec)/div, 50 ms/div

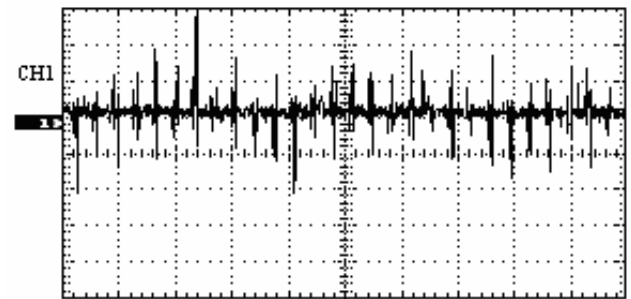


Fig. 16 (a)

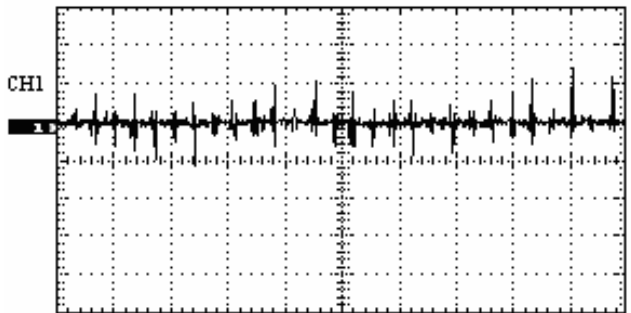


Fig. 16(b)

Experimental response of torque (a) MDTC. (b) ANN based DTC under steady state (0.5-Nm./div), 50 ms/div

VII. CONCLUSION

In this paper a new ANN based speed controller, flux position estimation, sector selection and the switching voltage vector selection has been proposed for direct torque controlled induction motor drive. The proposed scheme performance is compared with the modified DTC scheme under the steady state and dynamic conditions. According to the simulation and experimental results of a (3HP) test motor, amplitude of the stator flux ripple and developed torque ripple are reduced by notable amount with good speed dynamic. The both results support that the ANN based DTC scheme has better performance than modified DTC scheme. The feasibility and validity of the proposed identification have been proved by the excellent experimental results.

APPENDIX

The parameters of the three-phase Induction Motor, employed for simulation purpose, in SI units are

2.2 kW (3HP) Three phase 415V, 50 Hz, 1415 rpm,
 $R_s = 1.95 \Omega$, $R_r = 1.66 \Omega$, $L_{ls} = 244mH$, $L_{lr} = 243mH$,
 $L_m = 369mH$, $P = 4$, $J = 0.025 \text{ kg/m}^2$, $B = 1e-5 \text{ Nms}$

REFERENCES

- [1] F. Blaschke, "The principle of field orientation as applied to the new transvector closed-loop control system for rotating-field machines", Siemens Rev., 1972.
- [2] K. Hasse, "Zum Dynamischen Verhalten der Asynchronmaschine bei Betrieb Mit Variabler Standerfrequenz und Stander Spannung", ETZ-A, Vol. 89, No. 4, 1968, pp. 77-81.

- [3] Takahashi and T. Noguchi, "A new quick-response and high efficiency control strategy of an induction machine", IEEE Trans. Ind. Application., Vol. 22, Sep/Oct. 1986, pp. 820-827.
- [4] Takahashi and Y. Ohmori, "High-performance direct torque control of an induction motor", IEEE Trans. Ind. Application., Vol. 25, Mar./Apr. 1989, pp. 257-264.
- [5] L. M. Gnesiak, B. Ufnalski, "Neural Stator Flux Estimator with Dynamical Signal Preprocessing" IEEE Conf. (AFRICON 2004), pp. 1137-1142.
- [6] Rajesh Kumar and Santhosh Vijaya Padmanaban, "An Artificial Neural Network Based Rotor Position Estimation for Sensorless Permanent Magnet Brushless DC Motor Drive", IEEE conf. (IECON-2006), Nov. 2006, pp.649-654.
- [7] B.Kosko, "Neural Networks and Fuzzy Systems: A Dynamic Systems Approach to Machine Intelligence", Englewood Cliffs, NY Prentice Hall 1992.
- [8] B. K.Bose. "Neural Network Applications in Power Electronics and Motor Drives—An Introduction and Perspective", IEEE Trans. Ind. Elec., Vol 54, No. 1. 2007, pp. 14-32.
- [9] G. Cirrincione, M. Cirrincione, Chuan Lu, M. Pucci, "Direct torque control of induction motors by use of the GMR neural network" Int. Joint Conf. on Neural Networks Vol. 3, 20-24 July 2003, pp. 2106 – 2111.
- [10] P.P. Cruz, J.J.R. Rivas, "A small neural network structure application in speed estimation of an induction motor using direct torque control" IEEE Power Electronics Specialists Conf.(PESC. 2001) Vol. 2, June 2001, pp. 823 – 827.
- [11] M. Vasudevan and R. Arumugam "High – Performance Adaptive Intelligent Direct Torque Control Schemes For Induction Motor Drives", KMITL Sci. Tech. J. Vol. 5, July-Dec. 2005, pp. 559-576.
- [12] M. Ong, Dynamic Simulation of Electric Machinery Using Matlab/Simulink, (Prentice Hall, 1997).
- [13] Jun Hu and Bin Wu, "New Integration Algorithms for Estimating Motor Flux over a Wide Speed Range", IEEE Trans. on Power Electro. Vol. 13. No 5. Sept. 1998, pp. 969-977.
- [14] LiMin Fu, "Neural Networks in Computer Intelligence", (McGraw-Hill Inc., 1994), pp. 153-264.
- [15] S. Haykin, "Neural Networks - A Comprehensive Foundation", Prentice Hall, 1999.
- [16] F. J. Lin, J. C. Yu and M. S. Tzeng, "Sensorless Induction Spindle Motor Drive Using Fuzzy Neural Network Speed Controller", Electric Power Systems Research, Vol. 58, 2001, pp. 187-196.
- [17] Kukolj, F. Kulic and E. Levi, "Design of Speed Controller for Sensorless Electric Drives Based on AI Techniques: a Comparative Study", Artificial Intelligence in Engineering, Vol. 14, 2000, pp. 165-174.
- [18] M.T. Hagan and M. B. Menhaj, "Training Feedforward Networks with the Marquardt Algorithm", IEEE Trans. on Neural Networks, Vol. 5, No. 6, 1994, pp. 989-993.

BIOGRAPHIES



Rajesh Kumar received the B.Tech. degree in electrical engineering from the National Institute of Technology (NIT), Kurukshetra, India in 1994, the M. E. degree in electrical engineering from the Malaviya National Institute of Technology (MNIT), Jaipur, India in 1997 and the Ph.D. degree in Intelligent systems from University of Rajasthan, India in 2005. In 1995 joined as Lecturer with the Department of Electrical Engineering, MNIT, Jaipur and he is working as Reader in the same institute. His research interests include intelligent control, evolutionary algorithms, fuzzy and neural methodologies, power electronics, electrical machines and drives. Dr. Kumar received the Career Award for Young Teachers (CAYT) in 2002. He is a member of IEEE, member of Institute of Engineers (INDIA), member IETE, member IEANG and life member of Indian Society for Technical Education (ISTE).



R.A. Gupta was born in Chandera, Rajasthan, India, in 1956. He received B.E. (Electrical) and M.E. Degrees from the University of Jodhpur, India in 1980 and 1984, respectively. In 1982, he joined as an Assistant Professor in the Department of Electrical Engineering, University of Jodhpur. In November 1990, he joined as a Reader and become full Professor in 1999 at the Department of Electrical Engineering, MREC, Jaipur (INDIA). His field of interest includes power electronics, electrical machines and drives. Prof. Gupta is a fellow of Institute of Engineers (INDIA), a life member of (ISTE) and Indian Society for continuing Engineering Education



S.V. Bhangale was born in Malegaon village, Maharashtra, India in 1967. He received B.E. (Electrical) degree from SSGM College of Engineering, Shegaon, Amravati University, India in 1990 and M.E. from L.D. College of Engineering Ahmedabad, Gujarat University, India in 1993. In 1991 he joined as a lecturer in Department of Electrical Engineering Polytechnic, Shahada, India, Now working as a senior lecturer at Government Polytechnic, Dhule Maharashtra. He is a member of Institute of Engineers (INDIA), and a life member of Indian Society for Technical Education. At present he is research scholar at Malaviya National Institute of Technology (MNIT) Jaipur, India.. His primary area of research includes control of electrical machines.



Himanshu Gothwal was born on 21st August 1987 in Jaipur, Rajasthan. He is currently a Final year B.Tech student of Information Tech. at Malaviya National Institute of Technology, Jaipur, Rajasthan. His Area of interest is Neural Networks and Robotics